Spatial Array of Microwave Sensors for IoT-Based Wireless Connectivity

Seyi Stephen Olokede and Babu Sena Paul
Department of Electrical and Electronic Engineering Technology
University of Johannesburg, South Africa
solokede@gmail.com; bspaul@uj.ac.za

Abstract Spatial array of microwave sensors for IoT-based wireless connectivity is presented. The traditional challenges of poor input impedance matching associated with small antenna is analytically characterized using the many available formulae based on a novel 2 × 2 excitation network. Alternative microwave sensor solution designed at originally known low data throughput IEEE 802.11x standard, was previously investigated to support multi-channel bandwidth capacity, now examined for robust link budget to provide complementary leverage for IoT-based applications.

Keywords: Big data, insertion loss, integrated circuit, latency, parasitic effect, system-on-chip

1 Introduction

It is anticipated that internet of things (IoTs) would have grown considerably to become internet of all things in the next few decades. The growth is driven by the recent increase of smart homes, smart wearable devices, smart cars, smart cities, etc. Fundamentally, IoT-based technology require an efficient information management systems for low-cost data acquisition technique, effective data mining, process, collection and transmission. In most cases IoT eco-system, usually consisting of thousands of interconnected sensors, laptops, RFID tags, must be robust enough to generate, collect, communicate, and store these generated data securely without distortion or data loss. The transmission of these data to the local or cloud storage system must be through low-power wireless connectivity. Existing IEEE 802.11x wireless standard has been disadvantaged for highly densified IoT interconnection networks due to its power-hungry architecture, limited link budget, set-up difficulty, and, its cost ineffectiveness. Nonetheless, availability and adaption of its existing infrastructure as well as its user friendliness could make it a complimentary alternative as heterogeneous interconnected wireless connectivity for IoT, in particular, when an efficient low-power alternative radio connectivity is provided. In [1], we presented a novel microwave sensor whose form factor does not depend on the radiation wavelength, but rather on the lumped elements. The sensor was reducible to smaller aperture size with respect to the resonance. Because of this capability, the structure becomes miniaturized to mitigate its power hungry propensity. In this work, we intend to focus on the possibility of enhancing the link budget rather than estimate the power hunger property of the proposed design or to assess to what extent the hunger was been mitigated. We intend to consolidate on many of the advantages of the structure as identified in [1]-[2]. We have demonstrated that the structure when properly matched could deliver close to 17 bandwidth channels of 20 MHz each based on the IEEE 802.11 U-NII-3 standard, with link

budget of more than 9 dBi. We assume a better link budget could be achieved if an array is implemented provided good impedance matching can be attained. We therefore out of necessity investigate the input impedance matching as a precursor to establishing our set goal. We subsequently examine the effect of efficiently coupled proximity coupled array to enhancing the link budget.

2 Problem Formulation

Figure 1 depicts a typical IoT technology. The data are collected by the interconnected sensors, which in turn are transmitted to low-power, high-speed, large-scale, highly interconnected microcontroller (servers). Wireless networks such as BLE, Bluetooth, ZigBee, Wi-Fi, etc. are normally used to connect these thousands of sensor nodes to the gateway. However, the transmission of data from the transmitter to the cloud require high speed and long range wireless internet connectivity depending on the systemic requirement. This is the focus of this work.

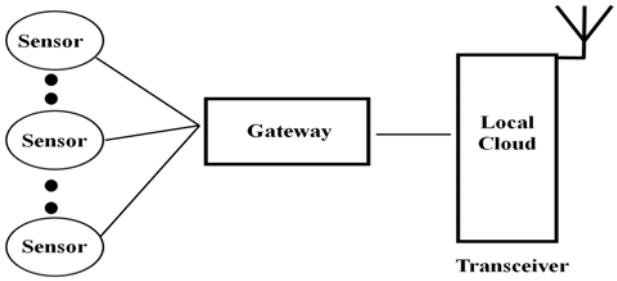

Figure 1: Typical Layout of IoT System

2.1 Input Impedance Matching

In Figure 2, the spatial array configuration to enhance both the channel bandwidth and the link budget in order to provide a robust platform for high data throughput is depicted. We assume that the depicted $m \times n$ array elements are optimally power-coupled by the excitation network. We provided $x \times y$ excitation network to ensure optimal coupling is guaranteed. We ensure that each element is identical and are at equidistance position in both x- and y-direction. We further map the array into sizeable rectangular sub-array lattices, such that array pattern of $\lambda/2$ inter-element spacing is maintained in both x-, and y-plane. We exited each sub-array lattice with an excitation source to ensure that each element is optimally power-coupled. On excitation, both magnetic and electric flux densities are created on the plane perpendicular to the plane where the array pattern are laid. The flux densities in turn excite the other array sensors via mutual and self-couplings. The equation to determine the mutual coupling is stated in matrices of equation (1).

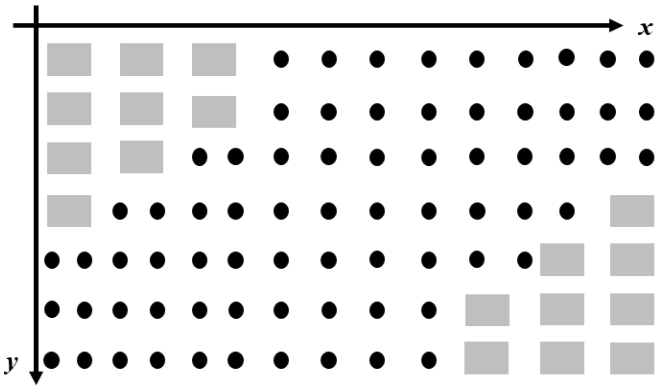

Figure 2: Spatial Array of microwave Sensor

$$Z_{Port1} = \begin{bmatrix} Z_{11}+Z_L & Z_{12} & Z_{13}..... & Z_{15} \\ Z_{21} & Z_{22}+Z_L & Z_{23}..... & Z_{25} \\ . & . & ..... & . \\ Z_{51} & Z_{52} & Z_{53}..... & Z_{55}+Z_L \end{bmatrix}$$

$$Z_{Port2} = \begin{bmatrix} Z_{65}+Z_L & Z_{66} & Z_{67}..... & Z_{65} \\ Z_{75} & Z_{76}+Z_L & Z_{77}..... & Z_{79} \\ . & . & ..... & . \\ Z_{105} & Z_{106} & Z_{107}..... & Z_{109}+Z_L \end{bmatrix}$$

$$Z_{Port3} = \begin{bmatrix} Z_{61}+Z_L & Z_{62} & Z_{63}..... & Z_{65} \\ Z_{71} & Z_{72}+Z_L & Z_{73}..... & Z_{75} \\ . & . & ..... & . \\ Z_{101} & Z_{102} & Z_{107}..... & Z_{105}+Z_L \end{bmatrix}$$

$$Z_{Port4} = \begin{bmatrix} Z_{65}+Z_L & Z_{66} & Z_{67}..... & Z_{65} \\ Z_{75} & Z_{76}+Z_L & Z_{77}..... & Z_{79} \\ . & . & ..... & . \\ Z_{105} & Z_{106} & Z_{107}..... & Z_{109}+Z_L \end{bmatrix}$$

. . .

(1)

The total input impedance (Z_{Total}) due to the mutual coupling is stated in equation (2). An array of 9 × 10 is configured such that the entire array is sub-divided into four 5 × 5 sub-array lattice and excited by a 2 × 2 excitation sources.

$$Z_{TOTAL} = \begin{bmatrix} Z_{Port(1,1)} & Z_{Port(1,2)} & ..... & Z_{(1,x)} \\ Z_{Port(2,1)} & Z_{Port(2,2)} & ..... & Z_{Port(2,x)} \\ . & . & ..... & . \\ Z_{Port(y,1)} & Z_{Port(y,2)} & ..... & Z_{Port(y,x)} \end{bmatrix} \quad (2)$$

The total input impedance as a result of the mutual coupling based on the four probes is as stated in equation (3). The input impedance is determined based on the scattering parameter coefficients, and are as stated in equation (4) [3].

$$Z_{TOTAL} = \begin{bmatrix} Z_{Port(1,1)} & Z_{Port(1,2)} \\ Z_{Port(2,1)} & Z_{Port(2,2)} \end{bmatrix} \quad (3)$$

$$\begin{bmatrix} b_1 \\ b_2 \end{bmatrix} = \begin{bmatrix} S_{11} & S_{12} \\ S_{21} & S_{22} \end{bmatrix} \begin{bmatrix} a_1 \\ a_2 \end{bmatrix}, \begin{bmatrix} b_1 \\ b_3 \end{bmatrix} = \begin{bmatrix} S_{31} & S_{32} \\ S_{41} & S_{42} \end{bmatrix} \begin{bmatrix} a_1 \\ a_3 \end{bmatrix}$$
$$\begin{bmatrix} b_3 \\ b_4 \end{bmatrix} = \begin{bmatrix} S_{13} & S_{14} \\ S_{23} & S_{24} \end{bmatrix} \begin{bmatrix} a_3 \\ a_4 \end{bmatrix}, \begin{bmatrix} b_2 \\ b_4 \end{bmatrix} = \begin{bmatrix} S_{33} & S_{34} \\ S_{43} & S_{44} \end{bmatrix} \begin{bmatrix} a_2 \\ a_4 \end{bmatrix} \quad (4)$$

The excitation voltage waves have been normalized using values a_1, a_2,……., and, b_1, b_2, …… Therefore, the respective currents and voltages as a function of excitation sources are stated in equation (5) and (6).

$$I_1 = \frac{1}{\left(Z_{Port1}\right)^{0.5}}\left(a_1 - b_1\right), \; I_2 = \frac{1}{\left(Z_{Port2}\right)^{0.5}}\left(a_2 - b_2\right)$$
$$I_3 = \frac{1}{\left(Z_{Port3}\right)^{0.5}}\left(a_3 - b_3\right), \; I_4 = \frac{1}{\left(Z_{Port4}\right)^{0.5}}\left(a_4 - b_4\right) \quad (5)$$

$$v_1 = \left(Z_{Port1}\right)^{0.5}\left(a_1 + b_1\right), \; v_2 = \left(Z_{Port2}\right)^{0.5}\left(a_2 + b_2\right)$$
$$v_3 = \left(Z_{Port3}\right)^{0.5}\left(a_3 + b_3\right), \; v_4 = \left(Z_{Port4}\right)^{0.5}\left(a_4 + b_4\right) \quad (6)$$

The total impedance (Z_{total}) is analyzed for a 2 × 2 excitation network using Matlab code. Figure 3 is the obtained total impedance (Z_{total}) with respect to inter-element spacing. Perfect matching was observed at Z = 0.5λ. Based on this, a proof of concept based on inter-element spacing of 0.5λ was designed using EM microwave HFSS Ansys solver. Figure 4 shows the obtained results.

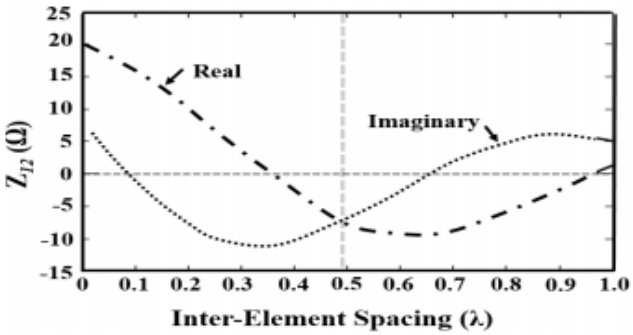

Figure 3: Transfer impedance vs. inter-element spacing

The input impedance is theoretically estimated to be 49.66 + j1.07 Ω, whereas, the HFSS simulated result indicate a value of 49.98 + j0.23 Ω. It is evident from the two results that the reactive component is very meagre. As such, the impedance match is considerable.

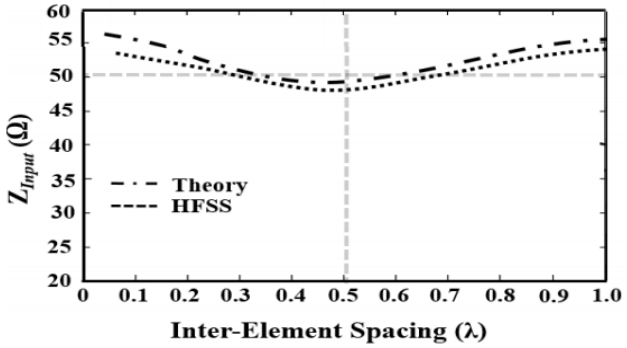

Figure 4: Input impedance vs. inter-element spacing

2.2 Link budget

The extracted values of the voltages and currents of equations (5) and (6) are applied to the array configuration for the purpose of the proof of concept. We assume that element factor $f(\theta)$ are identical due identical elements of the array, the inter-element spacing is uniform, and $f(\theta)$ is a function of the excitation sources, and also indirectly depend on the impedance matching emphasized in Section 2.1. Equations (7) indicates the current density for an excited microwave sensor, where $J_x(x, y)$ and $J_y(x, y)$ are as defined by equations (8) and (9), and N is equal to the number of inter-digit fingers. The electric field density per a sensor is stated in equation (10) [4]-[7].

$$J_z(z) = \sum_{i=n}^{N} \left(J_x(x,y) + J_y(x,y) \right) \tag{7}$$

$$J_x(x',y') = \frac{\cos\left(\frac{2\pi}{w_c}x'\right)}{\pi w_c\left(1-\left(\frac{2x'}{w_c}\right)^2\right)^{0.5}} \qquad n = 0,2,4,6,.....2n$$

$$\frac{\sin\left(\frac{2\pi}{w_c}x'\right)}{\pi w_c\left(1-\left(\frac{2x'}{w_c}\right)^2\right)^{0.5}} \qquad n = 1,5,7,9.....2(2n+1) \tag{8}$$

$$J_y(x',y') = \frac{\cos\left(\frac{2\pi}{w}y'\right)}{\pi w\left(1-\left(\frac{2y'}{w}\right)^2\right)^{0.5}} \qquad n = 0,2,4,6,.....2n$$

$$\frac{\sin\left(\frac{2\pi}{w}y'\right)}{\pi w\left(1-\left(\frac{2y'}{w}\right)^2\right)^{0.5}} \qquad n = 1,5,7,9.....2(2n+1) \tag{9}$$

$$E_z(x,y,z) = \int_{-\infty}^{\infty} G(k_z)E(R,z=0)e^{-jkz}dk_z \tag{10}$$

$$G(k_z) = \int_{-\infty}^{\infty} J_z(z)e^{-jkz}dk_z$$

where G(k_z) is the Fourier transform of the current distribution function upon excitation. The radiation far-field is stated as shown in equation (11). Therefore equation (11) can be decomposed to give equations (12) and (13) [8].

$$E^{Far-field} = \frac{E_z^{Array}}{\sin\theta}$$

$$E^{Far-field}(r,\theta,\varphi) = \frac{jk_0G(k_z)e^{-jkr}}{2nr} f_{(x,y)}(\theta,\varphi)\times 2\sum_{p(x,y)} I_pG(k_z)e^{jkr(x\cos\theta+y\sin\varphi)\sin\theta} \tag{11}$$

$$EP = \frac{jk_0G(k_z)e^{-jkr}}{2nr} f_{(x,y)}(\theta,\varphi) \tag{12}$$

$$AF = 2\sum_{p(x,y)} I_pG(k_z)e^{jkr(x\cos\theta+y\sin\varphi)\sin\theta} \tag{13}$$

where AF is the array factor, and EP is the product of the radiation intensities of the element. Equation 11 is the radiation pattern of the proposed $m \times n$ array.

3 Experimental Results

Equations (7) through to (13) were coded using Matlab, to firstly extract the required values to characterize the link budget of the proposed microwave sensor array. A proof of concept was realized based on the extracted values using 3D EM numerical finite integration technique code. The design is photoetched on Roger printed circuit microwave laminate board

3.1 Validation

To validate our proposition, an (9 × 10) array is implemented such that the array is sub-divided into (5 × 5) sub-array lattice as shown in Figure 2(a) of [2]. The (9 × 10) array is excited by (2 × 2) coaxial probe array coupling network, such that every (5 × 5) sub-array lattice is excited by at least one excitation source. Each microwave sensor is designed for IEEE 802.11 U-NII-3 standard, with resonance at 5.8 GHz. The inter-element spacing of 0.5λ is determined to be 14 mm where λ = 28 mm.

3.2 Results and Discussions

Figure 5 depicts the obtained normalized array factor (AF) based on equation (13) using Matlab code. It is evident that, the radiation pattern of the proposed array can be expressed as the product of the excited element factors $f(\theta)$ and the array factor (AF) i.e. AF × $f(\theta)$ as exemplified by equation (11) where $f(\theta)$ is expected to be identical for all the array elements. The obtained 3D AF plot is computed at θ = 90, and φ = 0 as shown in the Figure.

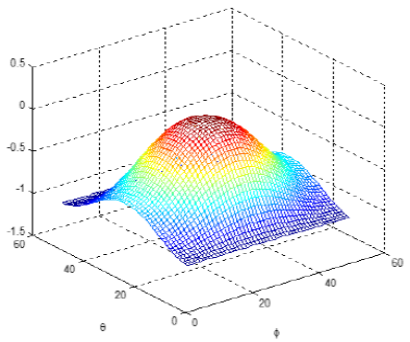

Figure 5: Obtained Normalized Array Factor (AF) of Equation (13)

Table 1 summarizes the obtained performance profile of the proposed design. Findings indicate firstly that the input impedance matching is substantial as demonstrated by considerable reflection coefficient $|S_{11}|$ of well over 30 dB, with superior voltage standing wave ratio (VSWR) of 1.081:1. The radiation efficiency is 69.18% and aperture efficiency is 72.80%. The proposed microwave sensor demonstrated a robust area occupancy of (2.7 × 2.4 × .0315)λ and a link budget of

about 20 dBi. The obtained link budget is very superior and can readily support long rage data transmission. The design is slim enough and are therefore adaptable for monolithic integrated microwave circuit.

Table I: Performance Profile of the Proposed Sensor

$\lvert S_{11}\rvert$ (dB)	VSWR	Freq (GHz)	Gain (dBi)	Radiation Efficiency (%)	Aperture Efficiency (%)	Aperture Size (mm)
34	1.081:1	5.80	19.79	69.18	72.80	$2.7\lambda \times 2.4\lambda$

4. Conclusion

In this paper, we presented spatial array of microwave sensors for IoT-based wireless connectivity for improved link budget. We opined that the IEEE 805.11x though have low data throughput could be used as complementary solution alongside the IEEE 805.15.4, in particular when efficient alternative solutions are provided to leverage on the interconnections of heterogeneous wireless networks. We demonstrated in our previous work that alternative solutions could demonstrate substantial channel bandwidth enhancement to support big data, and more so if they are interconnected. We went further in this work to prove that such could also achieve significant link budget if an array is implemented. We firstly demonstrated that a miniaturized microwave sensor is achievable at lower frequency spectrum, and secondly, showed that the prevailing impedance matching challenges of small antennas at lower frequency band is surmountable.

References

1. Olokede S.S, Paul B., (2016). “Miniaturized microwave sensor for internet of things wireless connectivity,” 16th Mediterranean Microwave Symposium, 14-16 November, Abu Dhabi, UAE. Accepted for publication
2. Ain, M. F., S. S. Olokede, Y. M. Qasaymeh, A. Marzuki, J. J. Mohammed, S. Srimala, S. D. Hutagalung, Z. A. Ahmad, and M. Z. Abdulla, (2013). “A novel 5.8 GHz quasi-lumped element resonator antenna,” *Int. J. Electron. Commun. (AEU)*, 67, 557–563.
3. Olokede S. S., and Adamariko C. A., (2015). "Analysis of the proximity coupling of a planar array quasi-lumped element resonator antenna based on four excitation sources," *Progress In Electromagnetics Research B*(63), 187-201.
4. Meixner, J. (1972). ”The Behaviour of Electromagnetic Fields at Edges. IEEE Transactions on Antennas and Propagation, 20(4), 442–446.
5. Olokede S. S., (2015). “A Quasi-Lumped Element Series Array Resonator Antenna,” Radioengineering, 24(3), 695-702.
6. Huang, F., Avenhaus, B., Lancaster, M. J. (1999). “Lumped Element Switchable Superconducting Filters. IEE Proceedings on Microwave, Antennas and Propagation, 146(3), 299–233.
7. Mittra, R., Lee, S. W. (1971). ”Analytical Techniques in the Theory of Guided Waves. McMillan. Aspin: B0006c0e1m
8. Simosvki, C. R. and S. He, (2001) “Antennas based on modified metallic photonic band gap structures consisting of capacitively loaded wires,” *Microwave and Optical Tech. Letters*, 31(3), 214–221.